Title
Accelerated Helium-Ion Beams for Radiotherapy and Stereotactic Radiosurgery

Authors
Ludewigt, B.
Chu, W.
Phillips, M.
et al.

Publication Date
1989-11-01

LBL-28280
Preprint

Lawrence Berkeley Laboratory
UNIVERSITY OF CALIFORNIA

Submitted for Publication

Accelerated Helium-Ion Beams for Radiotherapy and Stereotactic Radiosurgery

B. Ludewigt, W. Chu, M. Phillips, and T. Renner

November 1989

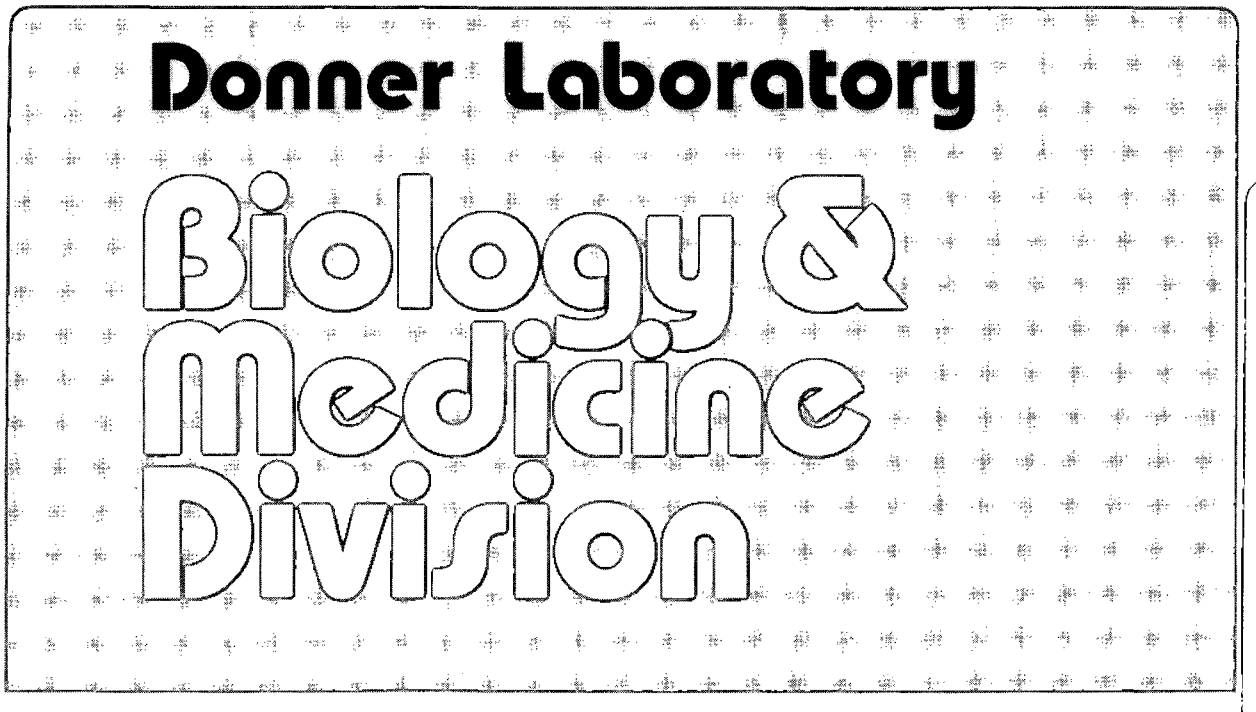

Prepared for the U.S. Department of Energy under Contract Number DE-AC03-76SF00098.

DISCLAIMER

Accelerated Helium-Ion Beams for Radiotherapy and Stereotactic Radiosurgery

B. Ludewigt, W. Chu, M. Phillips, and T. Renner
Lawrence Berkeley Laboratory, University of California, Berkeley, CA 94720, USA

Abstract

A new beamline for radiotherapy and radiosurgery with accelerated helium-ion beams has been set up at the Bevalac. The new treatment room has been equipped with a very precise patient positioner in order to utilize the superior dose localization properties of light ion beams. The beam spreading and shaping system is described, the tradeoffs involved in positioning the beam modifying devices are discussed, and the physical properties of the generated radiation fields are reported. The Bragg peak modulation by axial beam stacking employing a variable range shifter is explained and the control system including beam monitoring and dosimetry is presented.

1. Introduction

Heavy charged-particle beams, i.e., proton, helium-ion, neon-ion and heavier nuclei beams, are particularly well suited for the treatment of localized tumors and stereotactic radiosurgery due to their superior dose localization properties [1-4]. For many years helium-ion beams from the 184"-synchrocyclotron and neon-ion beams from the Bevalac accelerator complex at the Lawrence Berkeley Laboratory have been used for medical purposes.

Since the shut down of the 184" synchrocyclotron in 1988, the medical programs utilizing helium-ion beams have been continued at the Bevalac. The beam is produced by a duoplasmatron ion source and preaccelerated through a radiofrequency quadropole and an Alvaraz Linac before being injected into the synchrotron for the final acceleration [5,6]. The highest beam intensities at treatment room entrance are 2 x 10^{10} and 4 x 10^{10} particles per beam pulse (one pulse every four seconds) for the two beam energies per nucleon used (165 MeV and 235 MeV). The difference in beam intensity is due to different extraction and beamline transmission efficiencies for the two energies. The resulting dose rate depends on target volume and the utilization of the beam. However, the current clinical needs can be satisfied with the available beam intensities, which give dose rates of up to 5 Gy/min.

In order to facilitate the helium-ion programs at the Bevalac, a second treatment room and new patient facilities were built [7]. The accelerator complex can be switched within about 2 minutes from delivering neon ions to treatment room I to delivering helium ions to the new treatment room II so that treatments in these rooms can be interlaced.

Precise patient positioning is of the utmost importance for taking full advantage of the dose localization properties of helium-ion beams. The computer controlled and motor driven patient positioner ISAH (Irradiation Stereotactic Apparatus for Humans), which was used at the 184" synchrocyclotron [8], was moved to the new treatment room at the Bevalac and incorporated into the Biomed control system. The patient can be translated in 0.1 mm steps along three orthogonal directions and rotated in 0.1 degree steps around two axis.

The current medical programs at the Bevalac utilizing helium ions require three types of radiation fields. The smallest targets treated are tumors of the eye. They require a residual range and a spread out Bragg peak (SOBP) width of less than 3 cm. The lateral extension of the target volume is also less than 3 cm in diameter [9]. The range of the

beam particles has to be reduced by inserting material into the path of the ions since it is impractical to extract the beam from the Bevalac at the corresponding low energy. A total dose of about 10 Gy has to be delivered in a time short enough for the patient to hold the eye steady (max. ~ 2 minutes). The second field type was developed for the treatment of intracranial ateriovenous malformations (AVM) [10] and small tumors. The usable field size is 4 cm in diameter and the maximum range is about 15 cm. The third type provides fields up to 8 cm in diameter and residual ranges up to 25 cm for the treatment of tumors [11] and large AVM's. In the last two applications the typical dose delivered in one irradiation (one port, one fraction) is about 2 Gy.

Since the helium programs exploit the superb dose localization properties of heavy charged-particle beams, it is important to minimize the width of the lateral dose falloff (penumbra) and the distal falloff. The radiation field uniformity specification across the target volume is ±5% or better. The system needed to spread the beam, both, laterally and in depth, is discussed and described in this paper and the physical properties of the generated helium-ion fields are presented.

2. Beam Spreading and Shaping System

In designing a beam line with it's beam spreading and shaping system, the following parameters of the radiation field need to be optimized: field size, dose uniformity, dose rate, lateral edge sharpness, distal falloff, residual range, peak to plateau ratio, neutron production, and fragmentation. This leads to contradictory requirements necessitating tradeoffs and compromises as discussed below. For the generation of optimal radiation fields the placement of the various beamline elements is crucial.

2a. Field Size and Dose Uniformity

The beam as extracted from the accelerator and channeled into the treatment area is rather narrow, with a beam spot diameter of, typically, one to two centimeters. In order to produce radiation fields of clinically useful sizes, the beam has to be spread out laterally. This can be done in different ways. The simplest one uses a single scattering foil or plate. A higher Z material is preferred since it introduces more scattering and produces fewer nuclear reactions for a given amount of particle energy loss. This method leads to radiation fields with Gaussian intensity profiles. Since only the innermost part of the Gaussian with more than 90% of the peak intensity can be used to cover the target volume, corresponding to a minimum dose uniformity requirement of ±5%, the beam utilization is at best 10% and hence only small radiation fields can be generated in this

way. For large fields the double scattering method [12,13] or magnetic spreading methods like the wobbler system [14] or a raster scanner [15-17] have to be used. The magnetic methods can generate larger fields without beam degradation and with a beam utilization of more than 30%. Currently, at the Bevalac the larger target volumes are treated in treatment room I with the wobbler beam delivery system [14]. Fields of up to 30 cm in diameter with a 28 cm residual range can be produced. A set of two dipole magnets is being installed in treatment room II and will provide large uniform fields by raster scanning a small beam spot across the target area.

For the generation of small helium fields we have adopted a single scatterer system illustrated in Fig. 1. The vacuum beam pipe ends at the treatment room entrance where the beam's size and position are monitored by a wire chamber. This chamber is followed by a computer controlled device used to insert the desired amount of scattering material and a collimator which limits the beam diameter (see following section). Located downstream of it are two beam detectors, an ionization chamber and a secondary electron emission monitor (SEM), which measure the amount of beam delivered (see following section). The residual range for a particular treatment is adjusted with a variable-thickness water absorber. A second ionization chamber for dose monitoring and the patient collimator are located close to isocenter. Various large, circular collimators and an iron pipe were installed, as shown in Fig. 1, in order to shield the patient from scattered particles.

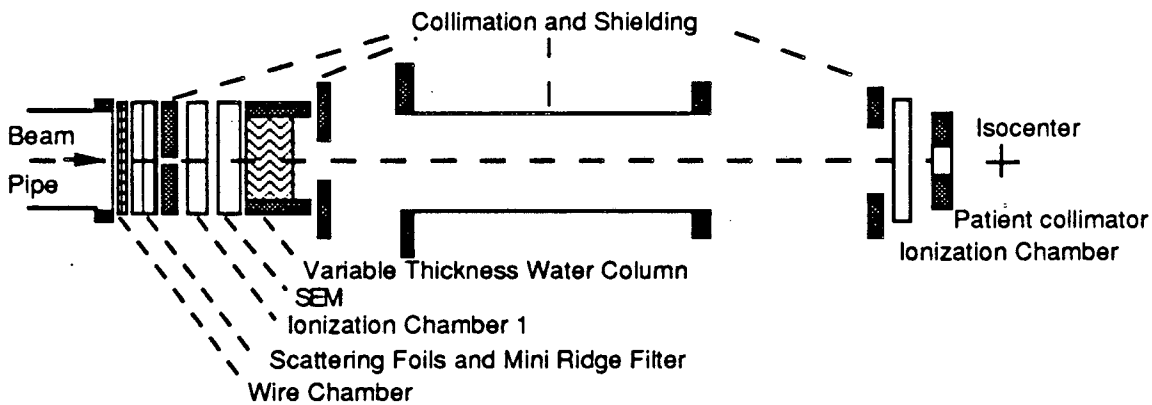

Fig. 1. Schematic of new helium beam port, not drawn to scale. Dimensions: Distance from end of beam pipe to isocenter is 6 m, the beam pipe diameter is 20 cm.

For the smallest radiation fields (ocular beams) no scattering material is inserted and the beam is spread only by the variable-thickness water absorber. For the largest

fields, 8 cm in diameter, a 1.2 cm thick brass plate is used for scattering. (see Table 1). The variable amount of water in the path of the beam introduces additional scattering, spreads the beam more and produces even flatter fields but, at the same time, lowers the dose rate due to the spreading of the beam beyond the target area. The usable field diameters are given in table 1 for zero water-thickness.

Energy per nucl (MeV)	Max. Range (cm)	Field Dia. (cm)	Scatterer	Range Shifter	Stacking Steps (cm)
165	15.5	4.0	miniridges	var. water	0.5
165	4.0	3.0	none	12.5 cm poly + var. water	0.3
235	25.0	8.0	1 cm brass	var. water	propeller, 0.3

Table1: Beam parameters.

2b. Lateral Dose Falloff

In order to take full advantage of the dose localization properties of heavy charged-particle beams, great care was taken to minimize the width of the lateral dose falloff. Besides the multiple scattering inside the patient body and the range-compensating material (bolus), which is unavoidable, the apparent, finite source size causing a half shadow can be a major contributor to the penumbra. In order to minimize the apparent source size, the diameter of the beam needs to be as small as possible where the beam traverses scattering material. Placing the scattering and range-shifting material upstream where the beam is not yet laterally spread can accomplish this [18].

We achieve a small source size and a good penumbra by focussing the beam on a wire chamber located about 6 m upstream of isocenter (Fig. 1) to a FWHM of less than 2 cm and by placing a collimator, which clips the tails of the Gaussian distribution, downstream of the scattering materials. The variable-thickness water absorber is located about 30 cm downstream of the collimator. The chosen aperture of 4 cm in diameter produces a satisfactory penumbra while more than 80% of the beam still passes through it. The solid line in Fig. 2 shows a typical beam profile with a 90% to 10% dose falloff of 2.5 mm as achieved by the described beamline setup. The dashed curve in Fig. 2 shows how the penumbra degrades due to the introduction of angular confusion when the range shifting material (water absorber) is moved closer to isocenter (from the position indicated in Fig. 2 to about 60 cm upstream of isocenter next to ionization chamber 2). Table 2 lists the width of the penumbra measured by

diode scans in a water phantom as function of the depth in water. The measured penumbra values are slightly higher then those reported in ref. 2,3. This can be attributed to the larger source size as defined by the 4 cm diameter aperture.

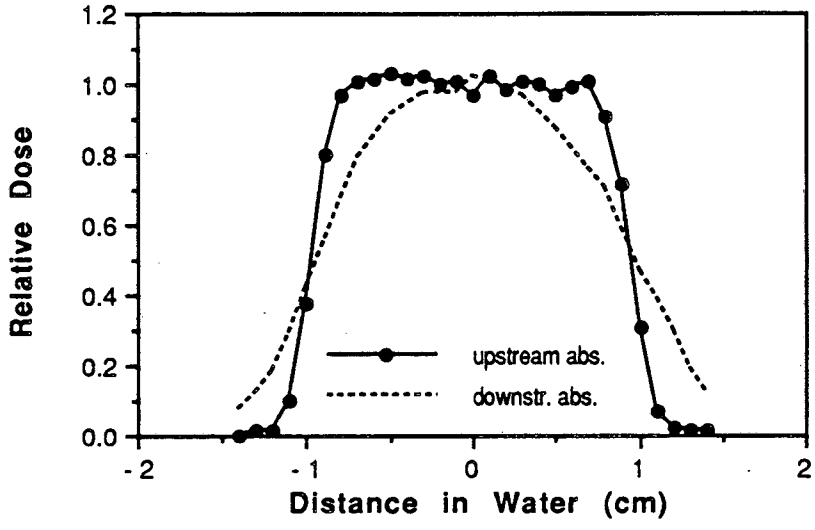

Fig. 2. Dose profiles at the center of a 2 cm spread-out Bragg peak (SOBP) at 6 cm depth in a water phantom as measured by a diode detector. The beam was shaped by a circular collimator with a 2 cm diameter aperture located 8 cm upstream of the water phantom (8 cm air gap). Solid curve: range shifting (absorber) material in upstream position; dashed curve: range shifting material in downstream position (see text).

The eye treatments require only short range beams and small fields but a very high dose rate. At the Bevalac the lowest practical helium beam energy per nucleon is 165 MeV and the range of the helium-ions needs to be reduced. The necessary amount of material in the beam introduces a significant beam divergence due to multiple Coulomb scattering. Depending on the position of the absorber material, this can lead to an intolerable increase in beam spot size and, therefore, a reduction in dose rate. In order to achieve the required dose rate of 5 Gy/min, we were forced to modify the above described arrangement of the beam modifying devices and to place 12.5 cm of polyethylene as range shifting material on the upstream side of the patient aperture. As can be seen in Fig. 3, which shows two beam profiles at different depths, the 90 % to 10 % dose-falloff is about 3.5 mm.

The closeness of the proximal peak to the eye's surface is a second reason for attaching the range shifting material directly to the patient collimator. It minimizes the scattering effect on the low velocity particles and, therefore, preserves the modulated Bragg peak shape.

Depth (cm)	Penumbra (90% - 10%) (mm)
6	2.5
9	3.5
12	4.5
17	7.0

Table 2: Distance between 90% and 10% dose points at midpeak of a 20 mm modulated stopping region (SOBP) as a function of depth in water. The collimator to water phantom distance is 8 cm.

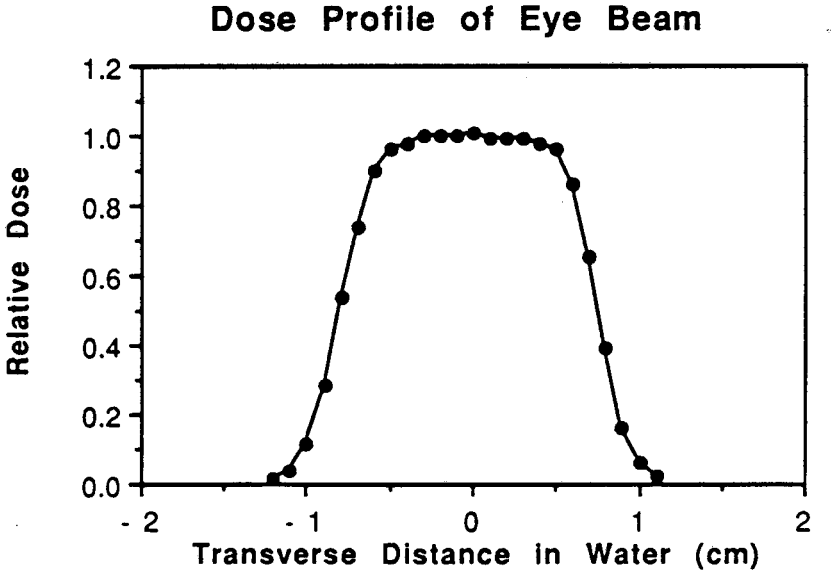

Fig. 3. Dose profile measured in water phantom. SOBP width: 2.0 cm, residual range: 2.5 cm, depth in water: 1.8 cm, collimator diameter: 1.5 cm, air gap: 4.0 cm.

2c. Other Radiation Field Parameters

In order to minimize neutron production and projectile fragmentation and to maximize the peak-to-plateau ratio of the spread-out Bragg peak, the minimal amount of material needed for scattering or for energy degradation should be inserted into the

beam's path. The position of the scattering and energy degradation material also affects the peak-to-plateau ratio. This ratio is slightly enhanced when the material is placed further upstream. For example, moving 9.5 cm of water absorber from a position 60 cm upstream of isocenter to 5 m upstream of it increases the peak to plateau ratio, as measured in a water phantom for a helium beam of an energy per nucleon of 165 MeV, by about 15%.

The sharpness of the Bragg peak and its distal falloff is determined by the energy resolution of the accelerator and the amount of range straggling introduced by the material in the beam's path. The width of the distal falloff of the modulated Bragg peak depends further on the details of the Bragg peak modulation which is discussed in the next section.

3. Bragg Peak Modulation by Axial Stacking

The narrow Bragg peak needs to be spread out in depth over the entire target volume, that is, the range of the beam particles needs to be modulated. This can be done by placing propellers or ridge filters [19,20], which cause the beam particles to lose part of their energy in various thicknesses of material, in the beam. Both devices are best located upstream where the beam diameter is small, thus reducing their size and minimizing their effect on the penumbra.

We have developed an alternative method for modulating the Bragg peak utilizing a variable-thickness water absorber to dynamically stack Bragg peaks in depth [21]. During the treatment the water-thickness is increased in steps, thus, achieving the same result as a propeller. Instead of delivering at any given time a mixture of range modulated particles, particles with different residual ranges are delivered sequentially. There are two main advantages of this method: first, the width of the SOBP can be varied in small steps without having to produce a large variety of propellers and, second, the amount of beam delivered at a certain depth and, therefore, the shape of the depth dose curve can be changed by simply varying the fraction of beam delivered at a particular depth. A disadvantage of the dynamic beam stacking is an increase in treatment time. This effect is moderate at the Bevatron since the time of three seconds between beam pulses is long enough to drive the water column to a new setting. Nevertheless, a time loss occurs whenever the requested amount of beam at a certain depth has been delivered before the end of a beam pulse. In that case the beam is cut-off with the rest of the pulse being lost. Depending on the total number of steps this can add up to half a minute over the course of a treatment.

We have implemented the dynamic beam stacking method for Bragg peak modulation for the treatment of small target volumes. Tumors of the eye are irradiated with unmodulated Bragg peaks stacked in 3 mm steps, which is the maximal step size that still yields a smooth depth dose distribution. Fig. 4 shows an example. The distribution is slightly sloped to give an isosurvival of about 1% (see next section). Mini-modulated or broadened peaks, which can be stacked in larger steps, are used for wider Bragg peak modulations. The mini-modulation is done by inserting a brass plate with triangular shaped ridges of 4 mm water equivalent thickness (mini ridge filter) into the beam. The resulting peaks can be stacked in 5 mm steps. An example of a depth dose distribution along the central axis and the predicted survival is shown in Fig. 5. The contributions of the single depth dose curves were adjusted as to give 10% isosurvival. The distal falloff can be significantly improved by adding a pristine Bragg peak at the distal end. An example is shown in Fig. 6.

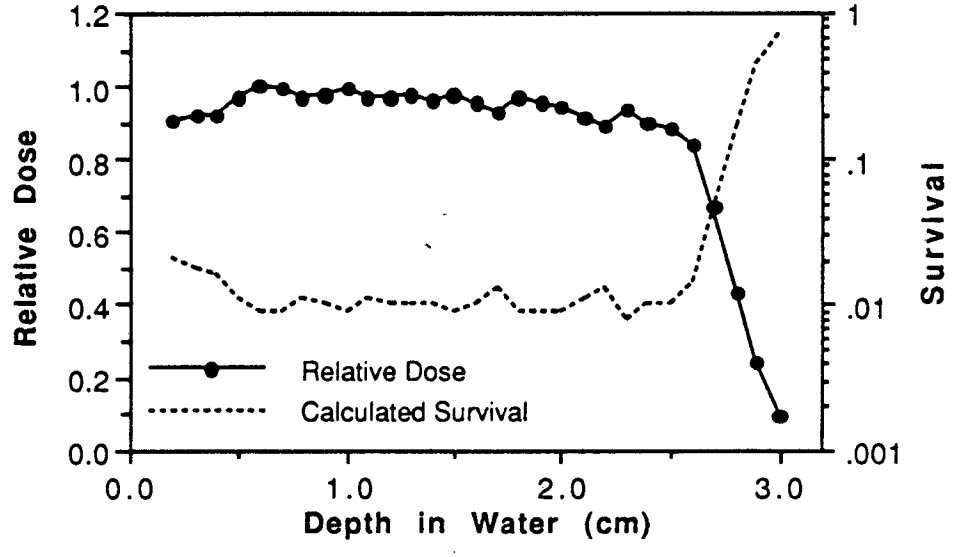

Fig. 4. Solid curve: depth dose distribution along central beam axis in a water phantom. Dashed curve: predicted (fitted) survival as function of depth. Pristine beams are stacked in 3 mm steps.

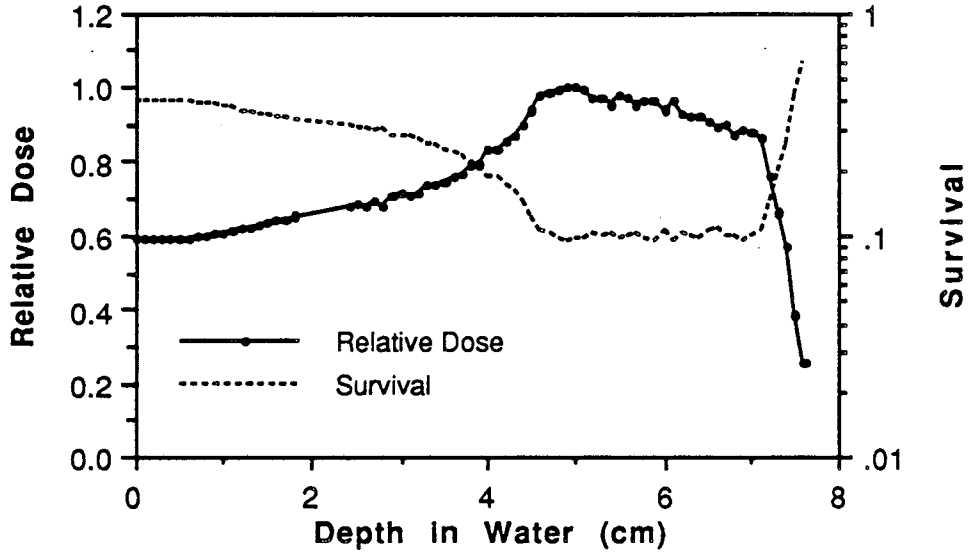

Fig. 5. Same as fig. 4. Mini-modulated beams are stacked in 5 mm steps for a 2.5 cm SOBP.

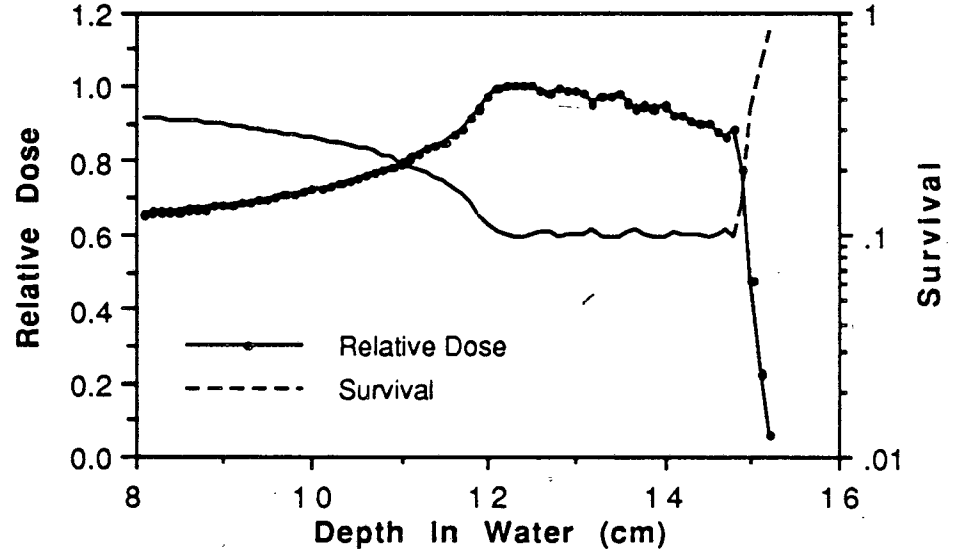

Fig. 6. Same as fig. 5, but in addition to the 6 mini-modulated beams a pristine peak is added at the distal end for a 2.7 cm SOBP.

4. Beam Weights

Beam weights are needed for propeller or ridge filter designs as well as for dynamic beam stacking procedures. Their values correspond to the fraction of beam particles of a certain range and are determined by a fitting procedure. For treatments with proton beams a uniform dose from the proximal to the distal end of the spread out peak is

usually desired and a straight forward optimization procedure can be applied to find a set of weights [19,20].

For heavier-particle beams, e.g., helium and neon beams, the efficiency for cell killing depends on the linear energy transfer (LET). Since the contribution of stopping particles increases from the proximal to the distal end of the peak, the dose average LET changes significantly across the spread-out peak and, consequently, the physical dose has to be decreased towards the distal end in order to achieve uniform cell killing. The linear-quadratic cell survival model [22,23] is employed to predict the cell survival at a given dose. The beam weights are determined by minimizing the difference between the desired and the calculated survival. They are treated as free parameters which are to be determined.

The family of depth dose distributions (Bragg ionization curves) used to determine the beam weights was found experimentally by measuring relative depth dose curves in a water phantom with a diode detector. The size of the diode and the accuracy of the positioning mechanism resulted in a position resolution of 1 mm. The depth dose curves were taken with exactly the same beamline setup as used for treatments and the particle range was varied by the same step size.

For calculating the cell killing an LET-value must be assigned to every point of the unspread depth dose curves. For the data presented in this paper this was simply done by using LET_∞-values from stopping power tables [24] up to a value of 150 MeV/(g/cm^2), which is reached at 2-3 millimeters residual range. The LET was assumed to stay constant at this value throughout the peak in order to take into account range straggling effects and the intentional Bragg peak broadening by the mini ridge filter. It should be noted that a crude model like this is at best applicable in cases where nuclear reactions and fragmentation are unimportant, such as for proton and short and medium range helium beams.

The cell survival S can be calculated in the linear-quadratic model if the coefficients α and β, which are a function of charge, mass and LET of the incoming particle, are known. Written as

$$S(LET,D) = \exp[-\alpha(LET)\ D - \beta(LET)\ D^2] \qquad (1)$$

for a particular particle type the model can be used to calculate the survival at a specific depth for stacked Bragg curves by expressing the dose D and the dose average LET as the sum of single Bragg curve distributions D_i:

$$D = \Sigma_i p_i D_i \quad \text{and} \quad \langle LET \rangle_D = [\Sigma_i p_i D_i LET_i]/D. \qquad (2)$$

The algorithm [25] used for calculating the coefficients α and β employs an empirical formula which is based on a collection of biological results [26,27]. The beam weights p_i are determined by minimizing the sum of the squares of the differences between the desired survival level S^o and the calculated survival S^j at all points, denoted by j, within the spread out Bragg peak. This can be written as

$$\text{MIN } (\Sigma [S^o - S^j(LET^j, D^j)]^2) \quad \text{with} \quad D^j = \Sigma_i p_i D_i^j. \qquad (3)$$

The fitted parameters p_i, when normalized ($\Sigma p_i = 1$), are the beam weights.

Using measured depth dose curves as input in the fitting procedure ensures the agreement of the measured modulated depth-dose curves with the expected ones for a given set of beam weights. The predicted survival is more uncertain due to the uncertainties in the dose average LET, in the beam composition and in the empirical parametrization of α and β.

The dynamic beam stacking method can be applied to heavier beams, longer ranges and larger modulation widths, but two improvements beyond the work described in this paper are needed. First, for heavier beams with larger nuclear reaction cross sections more sophisticated models, which take fragmentation effects into account [28,29] must be used for the calculation of dose average LET-values and beam composition. Second, the mini ridge filter has to be designed to optimize the width and the shape of the mini-modulated peak and has to be appropriately modeled for calculating the LET distribution.

5. Beam Monitoring and Dosimetry System

A wire chamber and a set of two plane-parallel ionization chambers are used for beam monitoring and dose measurement. The wire chamber consisting of two planes with 6 mm wire spacing for measuring the horizontal and the vertical beam profile is located at the beam entrance, where the beam is brought to a focal point. Two ionization chambers, one located upstream close to the wire chamber and the other one downstream close to isocenter, are used to define the beam axis. This is done by measuring the amount of beam collected on each quadrant of a circular collection foil. From the up/down and

left/right ratios one can precisely determine the beam position with respect to the chamber center [30,31,32]. A second collection foil is divided into concentric rings yielding information about the size and the intensity profile of the circular beam. The total amount of beam traversing the ionization chambers is measured by summing the quadrants. The number of beam particles is also monitored by a secondary emission monitor (SEM) [33]. This detector has the advantage, compared to the ionization chambers, that it does not saturate at the highest possible Bevalac beam intensities.

It is important to place all dosimeters (ionization chambers and SEM) downstream of the aperture which defines the beam spot size. In this position they see only the particles which contribute to the irradiation. The variable-thickness water absorber needs to be located downstream of IC1 and the SEM since it is used for adjusting the residual range and stacking the beam for the Bragg peak modulation. The second ionization chamber is placed 60 cm upstream of isocenter so that the delivered radiation can be monitored close to the patient.

The beam delivery is controlled by a VAX 780 computer using CAMAC hardware. The control system computer sets the beam modifying devices to their desired values, monitors them, reads out the ionization chamber dosimetry data, and initiates a beam cutoff when the treatment is finished or a failure has been detected. The part of the control system which relates to treatment room II is schematically depicted in Fig. 7. Taking the relevant information from a patient setup file, the computer inserts the correct amount of scattering material and sets the variable water column for the adjustment of the residual range. The patient positioner, ISAH, is also computer-controlled and the patient position is monitored during a treatment.

The beam is switched off by turning off (clamping) an extraction magnet when the desired dose at a particular range has been given. Such a clamp is initiated by preset scalers into which the expected number of counts, which corresponds to the total charge collected by each ionization chamber and the SEM, has been downloaded before irradiation. This is done at the beginning of the treatment and everytime before irradiating at a new water-column setting. Since the ionization chambers and the SEM do not directly measure the dose at isocenter, they must be calibrated for each residual range and SOBP width. For this purpose a reference thimble ionization chamber is placed at isocenter and the charge collected on the SEM and the ionization chambers signal foils per Gy delivered at isocenter as measured by the reference chamber is determined. When the Bragg peak is modulated by axial stacking, calibration factors are needed for each water column setting. After the treatment the delivered dose is determined by averaging

the three detector readings. Ionization chamber 1 and the SEM are weighted half as much as ionization chamber 2 since they measure the beam at the same location.

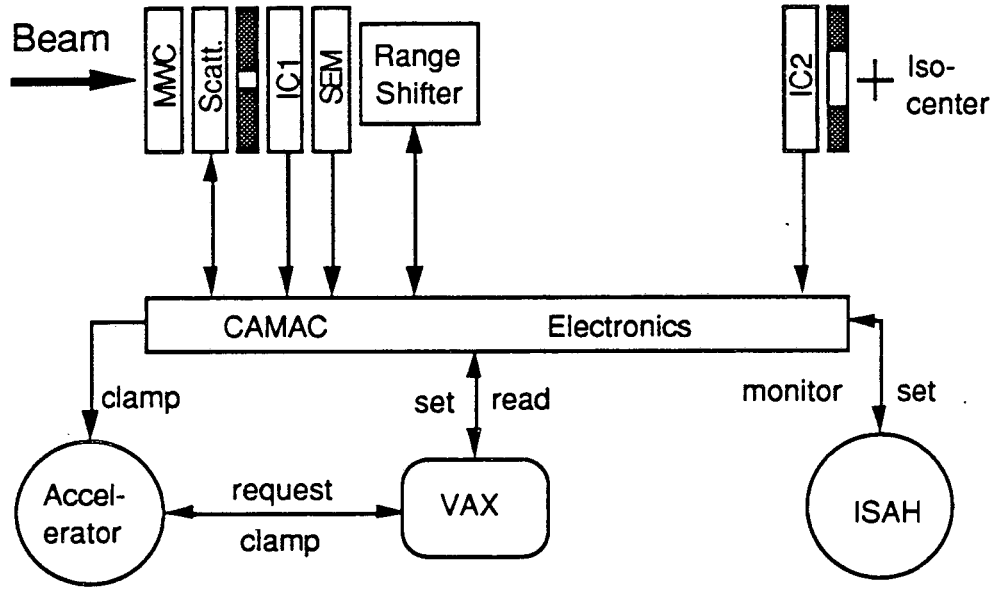

Fig. 7. Control and dosimetry system (schematic). MWC: multi wire chamber; IC1, IC2: ionization chambers; Scatt.: scattering foil and mini ridge filter inserter.

6. Summary

The helium beam line setup at the Bevalac with its single foil scattering system is well suited for the treatment of small lesions. It has been used for treatments of intracranial ateriovenous malformations and tumors of the eye for more than one year. The Bragg peak modulation by axial stacking of pristine or mini-spread peaks has resulted in a more flexible adjustment of modulation widths.

Acknowledgements

We would like to thank M. Nyman, R. P. Singh, and M. McEvoy for developing the control system hardware and software. We are very grateful to J. Lyman for making his subroutines for calculating the cell killing available to us.

This work was supported by the Director, Office of Energy Research, of the US Department of Energy under Contract no. DE-AC03-76F00098 and in part by the National Institute of Health under Grant CA 30236.

References

[1] G.T.Y. Chen, R.P. Singh, J.R. Castro, J.T. Lyman, J.M. Quivey,"Treatment planning for heavy ion radiotherapy." Int. J. Radiat. Oncol. Biol. Phys. 5, 1809-1819 (1979)

[2] J.T. Lyman, J.I. Fabrikant, K.A. Frankel,"Charged Particle stereotactic radiosurgery." Nucl. Inst. & Methods in Physics Research, B10/11, 1107-1110 (1985)

[3] J.T. Lyman, L. Kanstein, F. Yeater, J.I. Fabrikant, K.A. Frankel,"A helium-ion beam for stereotactic radiosurgery of central nervous system disorders." Med. Phys., 13, 695-699 (1986)

[4] C.A. Tobias,"Future of heavy ion science in biology & medicine." (Failla Memorial Lecture) Radiat. Res. 103, 1-33 (1985)

[5] J. R. Alonso," High Energy Heavy Ions: Techniques and Applications." Nucl. Inst. and Methods A244, 262 - 272 (1986)

[6] J. Staples et al., IEEE Trans. Nucl. Sci. NS-18, 538 (1971)

[7] J. R. Alonso, J. Bercovitz, W. T. Chu, B. Ludewigt, M. Nyman, R. P. Singh, R. Stradtner, R. Tafelski, and R. Walton,"Relocation of the Helium Ion Radiotherapy Program from the 184"Synchrocyclotron to the Bevalac." IEEE Trans. on Nucl. Sci., March 1989, Chicago,Ill.

[8] J.T. Lyman, C.Y. Chang, "ISAH: A versatile treatment positioner for external radiation therapy." Cancer 34, 12-16 (1974)

[9] W.M. Saunders, D. H. Char, J.M. Quivey, J.R. Castro, G.T.Y. Chen, J.M. Collier, A. Cartigny, E.A. Blakely, J.T. Lyman, S.R. Zink, and C.A. Tobias,"Precision High Dose Radiotherapy: Helium Ion Treatment of Uveal Melanoma." Int. J. Radiat. Oncol. Biol. Phys. 11, 227-233 (1985)

[10] J.I. Fabrikant, J.T. Lyman, K.A. Frankel,"Stereotactic heavy-ion Bragg peak radiosurgery: method for treatment of deep arteriovenous malformations." Br. J. Radiol. 57, 479-490 (1984)

[11] W.M. Saunders, G.T.Y. Chen, M. Austin-Seymour, J.R. Castro, J.M. Collier, G. Gauger, P. Gutin, T.L. Phillips, S. Pitluck, R.E. Walton, and S.R. Zink,"Precision, High Dose Radiotherapy. II. Helium Ion Treatment of Tumors Adjacent to Critical Central Nervous System Structures." Int. J. Radiat. Oncol. Biol. Phys. 11, 1339-1347 (1985)

[12] K. Crowe, L. Kanstein, J. Lyman, and F. Yeater,"A large-field medical beam at the 184-inch synchrocyclotron." Lawrence Berkeley Lab. Report No. LBL-4235,

1975

[13] A. M. Koehler, R. J. Schneider, and M. Sisterson,"Flattening of proton dose distributions for large field radiotherapy." Med. Phys. 4, 297 (1977)

[14] T. R. Renner, W. T. Chu, "Wobbler facility for biomedical experiments." Med. Phys. 14(5), 825 (1987)

[15] T. R. Renner, W. Chu, B. Ludewigt, J. Halliwell, M. Nyman, R. P. Singh, G.D. Stover,R. Stradtner,"Preliminary Results of a Raster Scanning Beam Delivery System." IEEE Trans. on Nucl. Sci, March 1989, Chicago, Ill.

[16] B. Larsson,"Pre-therapeutic physical experiments with high energy protons." Brit. J. Radiol. 34, 143-151 (1961)

[17] T. Kanai, K. Kawachi, H. Matsuzawa, and T. Inada,"Three-Dimensional Beam Scanning for Proton Therapy." Nucl. Instr. and Meth. 214, 491-496 (1983)

[18] M.M. Urie, J.M. Sisterson, A.M. Koehler, M. Goitein, J. Zoesman,"Proton beam penumbra: Effects of separation between patient and beam modifying devices." Med. Phys. 13(5), 734 (1986)

[19] B.G. Karlsson,"Methoden zur Berechnung und Erzielung einer fur die Tiefentherapie mit hochenergetischen Protonen gunstigen Dosisverteilung." Strahlentherapie 124, 481 (1964)

[20] A.M. Koehler, R.J. Schneider, and J.M. Sisterson,"Range modulators for protons and heavy ions." Nucl. Inst. Meth. 131, 437 (1975)

[21] K.H. Woodruff, J.T. Lyman, and J.I. Fabrikant, "Heavy Charged-Particle Induced Lesions in Rabbit Cerebral Cortex." Int. J. Radiat. Oncol. Biol. Phys. 14, 301-307 (1988)

[22] B. Fertil, P.J. Deschavanne, B. Lachet, E.P. Malaise,"In vitro radiosensitivity of six human cell lines. A comparison study with different statistical models." Radiat. Res. 82, 297 (1980)

[23] J.D. Chapman, E.A. Blakely, K.C. Smith, R.C. Urtasun,"Radiobiological characterization of the inactivating events produced in mammalian cells by helium and heavy ions." Int. J. Radiat. Oncol. Biol. Phys. 3, 97 (1977)

[24] W.H. Barkas and M.J. Berger,"Tables of energy losses and ranges of heavy charged particles. Studies in penetration of charged particles in matter." Natl. Acad. of Sci.-Natl. Res. Council, Publ. 1133 (1964)

[25] J.T. Lyman, priv. comm., 1988

[26] J.T. Lyman," Computer Modeling of Heavy Charged-Particle Beams." in: Pion and Heavy Ion Radiotherapy: Pre-Clinical and Clinical Studies. L.D. Skarsgard (Ed.),

Elsevier Science Publishing Co., Inc., pp. 139 (1983)

[27] J.T. Lyman,"Radiological physics consideration for selection of heavy charged-particle beams for biomedical research." In: Radiation Oncology, Maria Design Symposium, Vol. II, 27. Medical Accelerator Research Institute in Alberta, Edmonton, Alberta, Canada

[28] J.T. Lyman,"Heavy Charged-Particle Beam Dosimetry." in: Advances in Dosimetry for Fast Neutrons and Heavy Charged Particles for Therapy Applications, IAEA-AG-371/13

[29] S. B. Curtis,"Calculated LET Distributions of Heavy Ion Beams." Int. J. Radiat. Oncol. Biol. Phys., 3, 87 - 91 (1977)

[30] J.T. Lyman and J. Howard,"Dosimetry and Instrumentation for Helium and Heavy Ions." Int. J. Radiat. Oncol. Biol. Phys. 2 (Suppl. 2), 81-85 (1977)

[31] J.W. Boag in: Radiation Dosimetry, Vol 2, eds. F.U. Attix, W.C. Roesch and E. Tochlin (Academic Press, 1966) p. 11

[32] T.R. Renner, W.T Chu, B.A. Ludewigt, M.A. Nyman, and R. Stradtner, "Multisegmented Ionization Chamber Dosimetry System for Light Ion Beams." Nucl. Instr. Meth. A281, No. 3, 640 (1989)

[33] T.E. Burlin in: Radiation Dosimetry, Vol 2, eds. F.U. Attix, W.C. Roesch and E. Tochlin (Academic Press, 1972) p. 144

LAWRENCE BERKELEY LABORATORY
TECHNICAL INFORMATION DEPARTMENT
1 CYCLOTRON ROAD
BERKELEY, CALIFORNIA 94720